Chapter 3

P. falciparum infected RBCs in static cultures

First versions of INDISIM-RBC (see Section 2.2) have proved their validity to represent the mechanisms governing the propagation of *Plasmodium falciparum* in RBC *in vitro* cultures, as well as their capacity to provide understanding concerning the observed population dynamics (see Section 2.3). However, a more accurate description of the processes affecting the local environment of the RBCs is required when comparing different culturing devices (see Section 2.4).

The current chapter focuses on modeling the spatial structure of static *in vitro* culture systems. In particular, on how the geometrical characteristics of the hematocrit layer of settled RBCs influence the prevalence and the course of the infection. Firstly, the experiments carried out to explore different culturing setups are presented (Section 3.1). Secondly, the modifications on the 3D version of the Individual-based model are outlined and an abridged ODD description of INDISIM-RBC.*v3D* is presented (Section 3.2). Thirdly, some general results used to validate the 3D version of the simulator are put forward (Section 3.3). Finally, two underlying mechanisms that may cause the behaviour observed in real static *in vitro* cultures are analised: a) local limitations on the parasite proliferation (Section 3.4), and b) local degradation of the culture medium due to insufficient diffusion rates (Section 3.5). These potentially limitting factors are tackled through population-based models supported by the outcome of INDISIM-RBC.*v3D*.

3.1 Geometrical characterization of the static culture systems

3.1.1 Prelyminar considerations on the application of INDISIM-RBC.*v3D*

The initial steps in the modeling of any real system consists on finding an appropriate representation of the system under study. INDISIM-RBC correctly reproduces the observed behaviours of the cultures and apparently captures some of the underlying mechanisms of real system. It can be considered a good tool to simulate real systems.

The next step is applying the results of the model to better understand and control real systems. INDISIM-RBC.*v3D* is developed and used as a support tool to facilitate the analysis of different culturing setups with the aim of designing improved culturing devices.

In this sense, it is important to recall that one fundamental aim of the collaboration between MOSIMBIO and EMG-GSK was to use the models with practical purpouses. According to the EMG-GSK, the improvement of the *in vitro* culturing protocols initially followed two lines of investigation with different objectives:

1. One of the objectives was to better understand the factors and constraints on the static cultivation of malaria parasites in order to optimize its performance, better reproduce the conditions *in vivo* and interpret the results of drug trials.

2. The second objective was to develop an automated continuous suspension culture, an automatized bioreactor capable of maintaining steady conditions for the infected RBCs. Such an apparatus would be used to maintain the culture lines of different parasite strains and also serve to perform batteries of drug trials.

The results concerning line (1) were presented in Ferrer et al. (2008) and constitute the main part of this chapter. They comprise a systematic study on the constrains arising from the geometry of the haematocrit layer, which covers hematocrit layer depths that range from 0.06 mm to 3 mm, and a separation between the walls of the culturing device that varies from 7.5 mm to 9 cm.

The detailed study of experimental systems that differ only in their three-dimensional configuration demands the development of an explicit 3D model. The setting up of the version *v3D* required performing some additional measurements regarding the spatial structure of real static culture systems, both in the local scale (counting the number of multiply infected IRBC as an indirect measure of the propagation of the merozoite

in Section 3.1.2.1, or assessing the average RBC density within the hematocrit layer in Section 3.1.2.2) and at the level of description of the whole system (measuring the macroscopic geometry of the culture system and its effects, in Sections 3.1.2.3 and 3.1.2.4).

The research concerning line (2) led to preliminary considerations on the design of a prototype of a suspended cell airlift bioreactor. However, the model outcome suggested that suspension cultures required exploring new roads. The conclusions drawn from the application of INDISIM-RBC.*v3D* are similar to those presented in Section 2.3.6: a different set of rules for the interactions must be developed to deal with suspended cultures.

The research revealed that it is also beyond the scope of the model to deal with some technical limitations found in the agitated experimental systems. For instance, how to handle continuous subcultivation of the parasite (the model can not explain the observed loss of infection capability associated to this process) and how to control hematocrit and parasite leak through the filters and valves of the culturing device, among others. The study of suspension culture systems is left as a perspective for further work. Thus, the associated experimental trials are not presented here.

3.1.2 Experimental trials on static culture systems

The model in 3D attempts to capture the essence of the local environment of the RBCs, in order to analize how the spatial configuration of the static cultures affects the infection dynamics. For this reason, the following set of experiments have been carried out to get a more a detailed depiction of the hematocrit layer under typical culturing conditions.

3.1.2.1 Multiple infections in IRBCs

The simplest hypothesis regarding the invasion of RBCs by merozoites is to assume that it is an homogeneously random process, in the sense that every healthy RBC is equally susceptible to invasion. If this hypothesis holds, then the distribution of the number of malaria parasites per IRBC follows a Poisson distribution. However, if not all the RBCs are equally susceptible to invasion (i.e. if the pool of susceptible erythrocytes is smaller than the total number of RBCs, as occurs when the infection is a locally limitted process), the population of IRBCs must bear an increased number of parasites. The result is an increased proportion of multiparasited IRBCs, which implies that the distribution of the number of invasions per IRBC has a longer tail than the one predicted by the Poisson distribution (Simpson et al., 1999).

The Poisson distribution ($f_P(k;\lambda)$) expresses the probability of a number of events (k) occurring in a fixed period of time if these events occur with a known average rate (λ). It is given by:

$$f_p(k;\lambda) = \frac{\lambda^k e^{-\lambda}}{k!} \tag{3.1}$$

A corrected Poisson distribution function is used to analyse the experimental results. This is a Possion distribution that does not consider the probability of no events ocurring ($k = 0$). It can be used to tackle the distribution of the number of invasions within the populatiopn of IRBCs. The probability of no events ocurring can be associated to the population of non infected RBCs: $f_p(k = 0;\lambda) \sim 1 - \%I \sim 90\%$.

The observations of multiple infected parasites carried out by EMG-GSK (see Appendix B B.7) have been compared to the corrected Poisson distribution function (Figure 3.1).

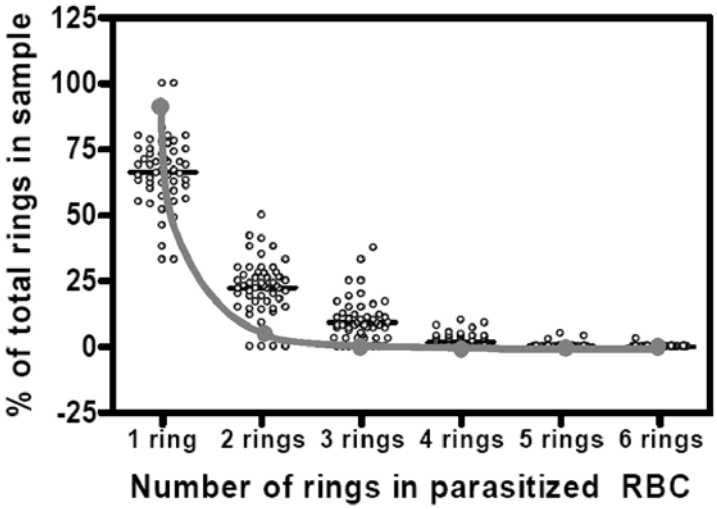

Figure 3.1: *Percentage of multiple infected RBCs. White dots (○): observed experimental counts in over 51 thin smears, each containing 2500 RBCs; grey dots (●) and solid line (-): theoretical ratio obtained with a corrected Poisson distribution assuming* $\lambda = 0.1$.

The parameter λ in the Poisson distribution represents the average number of parasites per RBC. Assuming a maximum threshold parasitaemia ($\%I = 10\%$), the expected number of parasites is $\lambda \sim 0.1$. The values obtained with a the corresponding Poisson distribution ($f_p(k;\lambda = 0.1)$ are significantly different to those observed in real cultures

(Figure 3.1). The correlation factor between observed and theoretical values is only $r^2 = 0.17$. More realistic parameters for the parasitaemia (i.e. $\%I < 10\%$) give worse fits. In conclusion, it can be stated that infection of RBCs is not a completely random process.

The measurement of multiple infected RBCs *in vitro* has been carried out to better understand the process of invasion of and to check the validity of the 3D-model for the local spreading of extracellular merozoites (see Section 3.3.3).

3.1.2.2 Cell density in the hematocrit layer

A determinant factor for the propagation of the infection in the model is the average distance between RBCs (see Section 2.3.6), which is related to the cell density in the hematocrit. The later is measured as the fraction of volume of the layer occupied by RBCs, *a.k.a.* RBCs average packing factor or just packing factor (pf).

Different culture devices are filled with culture medium plus healthy RBCs at 5% hematocrit, simulating an ordinary static culture. Their base surface (S) is small enough to allow an accurate measurement of the Hematocrit Layer Depth (HLD) and big enough to neglect capillarity effects. The real depth (HLD_{obs}) is measured once red blood cells are completely settled down. The depth expected if RBCs were completely packed without intersticial space (HLD_{calc}) is obtained through multiplying the culture depth (H_{total}) by the hematocrit fraction ($\%H = 0.05$). The real packing factor is calculated as the fraction of expected to real depths: $pf = \frac{HLD_{calc}}{HLD_{obs}}$. A description of the experimental methods is outlined in the Appendix B (Section B.6) the obtained results are shown in Table 3.1.

Culture device	$S\ [cm^2]$	$H_{total}\ [cm]$	$HLD_{calc}\ [cm]$	$HLD_{obs}\ [cm]$	pf
Glass 1	2.41 ± 0.05	8.7 ± 0.1	0.435 ± 0.005	0.5 ± 0.1	0.87 ± 0.17
Tube 1	0.50 ± 0.05	42.0 ± 0.1	2.1 ± 0.005	2.4 ± 0.1	0.88 ± 0.04
Tube 2	0.28 ± 0.05	66.5 ± 0.1	3.325 ± 0.005	3.9 ± 0.1	0.85 ± 0.02

Table 3.1: *Estimated RBC density within the hematocrit layer, according to the measurements using three different culture devices: glass 1, a flat bottomed test tube; tubes 1 and 2, plastic pipes similar to straws with a flat silicone seal at the bottom; S: base surface, calculated out from the measured diameter; H_{total}: measured culture depth; HLD_{calc}: expected depth of the hematocrit layer; HLD_{obs}: measured depth of the hematocrit layer; and pf: calculated packing factor of RBCs.*

The experimental RBC packing factor can be compared with the packing factors corresponding to theoretical spatial distributions of different objects. For instance, RBCs

can be approximated to rigid spheres with the same volume ($r_{sphere} = 2.71\ \mu m$). These spheres can be arranged in a perfectly ordered and optimally packed distribution, with all the spheres in contact one with each other and leaving minimum intersticial space between them. This spatial distribution corresponds to the so called Face-Centered-Cubic configuration (FCC). Its theoretical packing factor is known to be $pf_{FCC} \simeq 0.74$. Or else, spheres can be arranged in a random 3D distribution, but still placed so that each sphere is in contact with its inmediate neighbors (RS). This configuartion leaves some gaps between the spheres, and the resulting theoretical packing factor is $pf_{RS} \simeq 0.64$ (Berryman, 1983).

Alternatively, RBCs can be approximated to rigid disks of the same volume ($d_{disk} = 7.4\ \mu m$; $h_{disk} = 2\ \mu m$). They can be arranged in a perfectly ordered and optimally packed honeycomb-like distribution (HD), with a packing factor $pf_{HD} \simeq 0.91$. Instead, disks randomly packed in two dimensional layers in contact with each other (RD) give a packing factor of $pf_{RD} = 0.82$ (Berryman, 1983).

The packing factor observed in real cultures is $pf_{exp} = 0.87 \pm 0.07$. The observations are most consistent with the ordered placement of rigid disk-like RBCs. Such a resuslt tallies with the tendency of RBCs to form regular aggregate structures (ruleaux). Even so, a more disordered arrangement of RBCs is still compatible with observations in real cultures, if we consider RBCs as non-rigid bodies, that can be distorted to better fit one with each other.

The experimental results provide additional information: increasing HLD does not lead to an increase in the packing factor. This supports the hypothesis that there is no compacting of the hematocrit layer due to hydrostatic effects. It can be assumed that pf_{exp} remains constant throughout the haematocrit layer, no matter the value of HLD. This lack of compacting hypothesis is also compatible with theoretical arguments indicating that the net weight of the settled RBCs over any single cell is negligible when compared both to the cellular stiffness (Shung et al., 1982; Godin et al., 2007) and to the interactions among RBCs (Hochmuth and Marcus, 2002).

3.1.2.3 Shape of the hematocrit layer

The hematocrit layer and the free culturing medium behave as distinct phases in static cultivation: as long as the culture is not stirred, hematocrit and medium are regions with distinguishable physical properties. This comes together with the observation of a phenomenon typically associated to the surface tension of liquids: the formation of hematocrit puddles and the appearence of a meniscus in the interface between the hematocrit, the free medium and the walls of the culture vial.

The real shape of the hematocrit layer observed for certain geometries of the culturing vial is not strictly a thin flat deposit that covers all the bottom of the culturing device. On a (non-wettable) glass surface, small volumes of culture show haematocrit layers that ressemble a puddle and cover only a fraction of the total surface of the culturing device. In plastic culture vials (wettable surface), the hematocrit may stick to the walls and form a meniscus (see Figure 3.2). This observed behaviour can be explained as follows.

Both healthy and infected RBCs are subject to some extent to cell-to-cell attractive interactions: rouleaux and other kinds of RBC-RBC aggregates provide an adhesion energy per unit surface (γ) estimated to be $\gamma_{RBC} = 1 \cdot 10^{-4} \frac{N}{m}$ (Hochmuth and Marcus, 2002). The increased adhesivenes of IRBCs caused by knobs, which is exhibited in the formation of rosettes, contributes to increase this stickiness (Chotivanich et al., 2000). The intercellular attraction produces a net inward pull on the cells placed on the border of the hematocrit, which can be measured as a surface free energy (Foty and Steinberg, 2005).

Surface free energy (*a.k.a.* surface tension) resulting from mollecular interactions is used in physics to describe the behaviour of different phases of liquids. This analogy with liquids can be extended to define a capillary length (L_C): $L_C = \sqrt{\frac{\gamma}{g \cdot \rho}}$, where ρ is the density of the liquid, and g is gravity. L_C is the characteristic length scale in which intercellular interactions are comparable to gravitational energy. It defines the shape of the puddles of liquids, as well as the extent of the observed meniscus.

An estimation of the order of magnitude of the L_C corresponding to the hematocrit can be carried out assuming that the surface free energy between the hematocrit and the culture medium is $\gamma_{H20} \sim 1 \cdot 10^{-1} \frac{N}{m}$, and that the value of L_C of the culture medium is $L_c(H_2O) \sim 2\ mm$. This results in:

$$L_C(RBC) = \sqrt{\frac{\gamma_{RBC}}{\gamma_{H_2O}}} \cdot L_C(H_2O) \sim 0.06\ mm \tag{3.2}$$

L_C determines the maximum depth that the hematocrit layer can reach when RBCs are settled forming a puddle in the bottom of a glass vial without contacting its walls. It can be used to calculate the culturing surface (S) for small volumes of the hematocrit cultured in big vials. L_C is also associated to the range of the meniscus, where the hematocrit layer is affected by the presence of the walls of the culturing device. It can be used to interpret the effect of the distance between walls in static cultures.

The usual static culturing conditions imply dimensions much bigger than the capillary length, thus hematocrit layer may be considered a flat thin bed. Then, HLD is calculated from the total culture volume (V), the hematocrit concentration ($\%H$), the observed

culturing surface and the fraction of the hematocrit layer occupied by RBCs (pf).

$$HLD = \frac{V \cdot \%H}{S \cdot pf} \tag{3.3}$$

This calculated HLD is used to characterize the effect of the thickness of the hematocrit layer on the parasite development in static *in vitro* cultures with different surfaces and volumes.

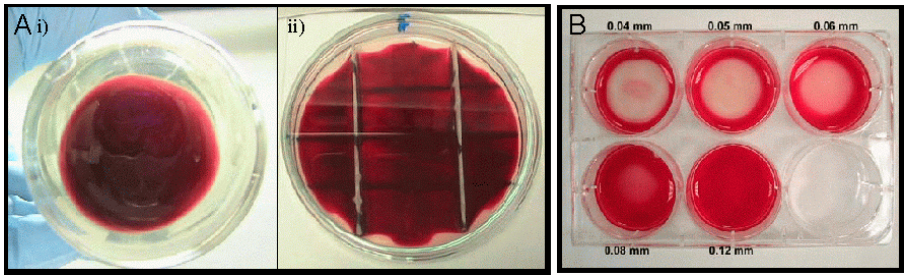

Figure 3.2: *Observed shape of the hematocrit layer in static culture systems. A) Glass culturing devices produce a convex meniscus. i) flat bottomed bottles used in the experiment* B *series. ii) petri dishes with plastic separators used in the* P *series (two separators). B) Plastic culturing devices produce a concave meniscus. Six-well plates used in the* W *series.*

3.1.2.4 Effect of the geometry of the hematocrit layer on the infection course

Static cultures are often referred to as 'thin-layer cultures', yet the exact meaning of 'thin' is not specified. Standardized protocols recommend two types of static *in vitro* cultures to carry out the *candle-jar* technique (MR4, 2008):

i) $V \sim 4\ ml$ with $\%H \sim 5\%$ in plastic flasks with a base surface $S = 25\ cm^2$, and

ii) $V \sim 12\ ml$ with $\%H \sim 5\%$ in flasks with $S = 75\ cm^2$.

If RBCs are settled in a perfectly compact layer, the thicnkess of the hematocrit layer is $HLD = 0.09\ mm$.

In most of the culturing protocols found in literature, the hematocrit layer depth is not explicitly defined. Its calculated value ranges from $HLD \sim 0.2\ mm$ (in the *candle-jar* method: $V = 1.5\ ml$, $\%H = 10\%$, $S \simeq 10\ cm^2$ and $pf \simeq 0.85$) to $HLD \sim 1.2\ mm$ (in cultures in alliquots: $V = 0.5\ ml$, $\%H = 10\%$, $S \simeq 1.5\ cm^2$ and $pf \simeq 0.85$) (Trager, 1994).

For the smallest cultures, HLD is only one order of magnitude greater than the characteristic length of RBCs (the diameter of the erythrocyte is $d_{RBC} = 6 - 8\ \mu m \sim 1 \cdot 10^{-2}\ mm$). In consequence, the HLDs proposed in literature represent significantly different backgrounds from the RBCs point of view. Such differences in HLD may be extremely important if the processes ocurring at a local level (e.g. uptake of nutrients, local spreading of the parasites, etc.) are limiting factors to the propagation of the infection.

The base surface of the culture systems found in literature also varies from trial to trial, ranging from $S = 1.5\ cm^2$ to $S = 75\ cm^2$. In this case, the dimension of the system is always several orders of magnitude grater than the characteristic length of the RBC, so the relative differences at the RBC scale are not so evident.

No systematic studies of the influence of the dimensions of the hematocrit layer on the parasite development have ben found in literature. The effect of the dimensions of the hematocrit layer on the culture performance (parasitemia $\%I$ and growth ratio GR) is analysed through three series of experiments performed by EMG-GSK. *Plasmodium falciparum* infected RBCs static *in vitro* cultures are raised under similar culturing conditions and different geometric characteristics. The trials compare different base surfaces, culture volumes and shapes of the culture vials. Their performance is parasitaemia and daily growth ratio is measured. They comprise three different experimental series, namely:

P-series) 2-day culture trials covering a range of base areas after fixing both the haematocrit layer volume and depth. They are carried out to evaluate the effect of the walls of the culture device. Cultures are set in glass Petri dishes, which have been previously split into dettached subregions by gluing plastic separators onto the plate base surface. Different distances between the glass separators (L) are trialed. The growth ratio at each subregion within a plate is evaluated separately. Each plate has a control subregion with a fixed surface to rule out differences not associated to the variation of L.

W-series) 14-day trials varying the hematocrit layer depth by modifying the total culture volume with a fixed base surface. They are carried out to evaluate the effect of HLD. Cultures are set in plastic trays, each containing 6 culture wells, and use small culture volumes (from 1 ml to 10 ml) .

B-series) 18-day trials varying the hematocrit layer depth (HLD) by modifying both the total culture volume (V) and the culturing surface (S). They are carried out to evaluate the effect of HLD and of the total culture volume. Cultures

are set in flat-bottomed glass bottles and use large culturing volumes (from 2 ml to 100 ml).

The geometric characteristics of the experimental sets are depicted in Figure 3.2. They are also presented together with the experimental results in Tables 3.2 and 3.4. Specifications of the culture methods are detailed in Appendix B, Sections B.8, B.9 and B.10.

Trial name	V (ml)	V_{RBC} (μl)	L (cm)	S (cm^2)	V_H (μl)	HLD (mm)	p (%)	R_{48}
P1	16.5	825	0.75	6.8	129.2	0.19	0.35 ± 0.19	0.6 ± 0.8
P2	16.5	825	1	9.0	171.0	0.19	0.6 ± 0.2	1.3 ± 0.8
P3	16.5	825	2	16.0	304.0	0.19	0.7 ± 0.4	2.2 ± 2.1
P4	16.5	825	4	32.0	608.0	0.19	0.9 ± 0.3	3.3 ± 1.6
P5	16.5	825	9	63.6	1208.4	0.19	1.2 ± 0.5	4.1 ± 1.5

Table 3.2: *Macroscopic geometric characteristic parameters and experimental results of the trials to assess the effect of the distance to the walls of the device on parasite development. P5 is the control plate with no internal walls. V refers to the measured total culture volume, V_{RBCs} refers to the calculated volume of packed RBCs and V_H refers to the calculated volume of the hematocrit layer. L refers to the measured distance between separators and S denotes the calculated base surface. HLD is the calculated depth of the hematocrit layer. p is the average observed parasitaemia and R_{48} is the calculated growth ratio at 48 hours. Reprinted from Ferrer et al. 2008, Malaria Journal* 7: 203.

Trial name	V (ml)	V_{RBC} (μl)	D (cm)	S (cm^2)	V_H (μl)	HLD (mm)	$\%I$ (%)	GR_{48}
W1	1.0	49.4	3.5	9.62	73.73	0.060 ± 0.015	1.5 ± 1.2	5.2 ± 1.8
W2	1.5	74.1	3.5	9.62	110.60	0.09 ± 0.02	1.6 ± 1.1	5.4 ± 1.9
W3	3.1	155.5	3.5	9.62	194.03	0.19 ± 0.05	1.7 ± 1.3	6 ± 2
W4	5.8	290	3.5	9.62	232.09	0.34 ± 0.08	1.5 ± 1.0	4.9 ± 1.0
W5	10.0	500	3.5	9.62	388.06	0.59 ± 0.15	1.4 ± 1.0	5 ± 2
B1	2.6	130	3.1	7.54	432.84	0.18 ± 0.05	1.8 ± 1.2	6.3 ± 1.2
B2	5.2	260	3.3	8.55	432.84	0.34 ± 0.08	1.7 ± 1.2	6.4 ± 0.9
B3	5.8	290	3.4	9.08	746.27	0.32 ± 0.08	1.7 ± 1.6	7 ± 3
B4	10.1	506.5	3.6	10.18	755.97	0.56 ± 0.14	1.4 ± 0.8	5.1 ± 0.8
B5	10.4	520	3.5	9.62	776.12	0.60 ± 0.15	1.4 ± 1.0	5.1 ± 1.8
B6	20.8	1040	3.9	11.94	1552.24	1.0 ± 0.2	1.1 ± 1.5	3.3 ± 0.7
B7	26.0	1300	4.1	13.20	1940.30	1.1 ± 0.3	1.0 ± 0.4	3.0 ± 0.5
B8	51.5	2074	5	19.63	3841.79	1.5 ± 0.4	0.7 ± 0.2	1.6 ± 0.3
B9	68.6	3432	5	19.63	5122.39	2.0 ± 0.5	0.50 ± 0.19	1.6 ± 0.6
B10	74.1	3705	5	19.63	5529.85	2.2 ± 0.5	0.4 ± 0.2	1.0 ± 0.6
B11	98.8	4940	5	19.63	7373.13	2.9 ± 0.7	0.3 ± 0.16	0.8 ± 0.4

Table 3.4: *Macroscopic geometric characteristic parameters and experimental results of the trials to assess the effect of HLD on the culture development. V refers to the measured total culture volume, V_{RBCs} refers to the calculated volume of packed RBCs,* and *V_H refers to the calculated volume of the hematocrit layer. D refers to the measured diameter of the hematocrit layer deposit and S denotes the calculated base surface. HLD is the calculated depth of the hematocrit layer. $\overline{\%I}$ is the average of the observed parasitaemias and $GR_{48}$is the calculated growth ratio at $48\,h$. W refers to cultures in 6-well plastic plates and B to cultures in $5\,cm$ diameter flat-bottom glass bottles. W assays with volumes lower than $1.0\,ml$ have not been presented because they did not develop well, due to the effects of surface tension. Reprinted from Ferrer et al. 2008, Malaria Journal* 7: 203.

3.2 ODD Description of INDISIM-RBC in 3D

3.2.1 Need for a 3D model

The results obtained with versions *2Dv.1* and *2Dv.*2 show that the model can be improved to better reproduce some features observed in real cultures.

The need of imposing a maximum threshold to the number of parasites that can invade a single RBC (Section 2.3.3) claims for improving the model of the propagation of extracellular merozoites through the hematocrit layer.

The absence of diffusive limitations that may cause the local exhaustion of medium in closed systems (Section 2.3.5), and which could explain the differences found between static and agitated cultures (Section 2.3.6), demands revisting the model of substrate diffusion.

The detailed study of different experimental static cultures also estimulates the development of INDISIM-RBC.*v3D*. The aim is to compare and understand the different performances observed in culture systems that are distinguished only through differencs in their geometry.

A description of the model is outlined below, following the scheme of the ODD but detailing only the specific modifications of this version. The complete description of INDISIM-RBC is found in Section 2.2.

3.2.2 ODD description of the 3D model

Overview

Purpose:
The model aims to decipher how the spatial structure of the hematocrit layer affects the static *in vitro* cultivation of *Plasmodium falciparum* IRBCs.

Entities and state variables:
Two low level entities are those defined in the 2D versions, the RBC and the spatial cell (*sc*). Their characteristic variables remain unaltered. The sole modification attains the extracellular merozoites. In the current version merozoites are tackled one by one, still they are not considered as individual entities because they do not have individual characteristics beyond their time spent in the extracellular medium and their position in the spatial grid (Grimm, 1999).

Characteristic scales:
The model is spatially explicit and stands for a small patch of the hematocrit layer. In this version (*v3D*), the space is modelled as a regular 3D grid formed by $I \times J \times K$ spatial cells, tipically, with $I = J = 20$ *sc* and $K = 40 - 1000$ *sc*. Each spatial cell is a square of $l_{sc} = 5$ μm side. Therefore, the whole grid represents a columm with a base surface of 0.01 mm^2 and a depth slightly bigger than the thickness of the hematocrit layer (HLD). Processes are modelled discretely and events take place at finite time steps. The time step (*ts)* is set to 1 hour. The value of the simulation unit that represent substrate particles (*su*) is set to 10^6 molecules.

Boundary conditions:
The fraction of the culture system included in the model is a column of the hematocrit layer and a small fraction of the culturing medium that covers it, the extent of the Diffusion Boundary Layer (DBL). Therefore, the limiting surfaces of the model have different boundary conditions.

i) *Top boundary:* The upper layer of spatial cells represents the free culturing medium. Bulk medium can be considered as an infinite source of glucose and a reservoir for lactate during the spans between two successive subcultivations. For this reason, top cells are considered as a closed boundary, meaning that they exchange substances only with side and lower spatial cells, and still maintain a substrate concentration fixed to the initial values: $C_{gluc}(i, j, HLD + DBL; t) = C_0$ and $C_{lact}(i, j, HLD + DBL; t) = 0$.

ii) *Bottom boundary:* The lower layer of cells lies on the surface of the culturing device. Bottom cells are considered a closed boundary that may accumulate the substrate, waste and deposits that settle down the hematocrit layer

iii) *Side boundaries:* Tipically, the modelled fraction of the culture system is placed in the midle of the hematocrit layer, so it is surrounded by almost replicas of the model. For this reason, the cells of the side surfaces are characterized with Periodic Boundary Conditions (PBC).

Eventually, side boundaries are considered a closed boundary to represent the effect of the side walls of the culturing device.

A depiction of the characteristic scales, entities and spatial structure of the model is depicted in Figure 3.3. The list of variables, their values (in simulation units and measured values) and the reference to the reference source to set them are presented in Table 2.1.

Process overview and Scheduling:
The general procedure and scheduling of *v3D* are the same as in versions *2D* (see Section 2.2).

Design concepts

The design concepts stated at Section 2.2 remain unaltered, except for the observation of the model outcome.

Figure 3.3: *Depiction of the entities, variables and spatial structure of the 3D versions of INDISIM-RBC.*
a) Side view of an experimental static culture, according to the MR4 protocol: i) controlled athmosphere, dimensions of the culture vials $D \sim 3$ *cm ii) free culture medium, depth of the culture* $H \sim 5$ *mm, iii) hematocrit, iv) modeled fraction of the culture system; b) spatial model of the hematocrit in 3D, measures* $X \times Y \times Z$, with $X = Y = 0.1$ *mm* and $Z = HLD + DBL$, *v) boundary layer, measures* $DBL \sim 0.1$ *mm, vi) hematocrit layer, its depth ranges* $0.1\ mm < HLD < 2\ mm$, *vii) top layer: reservoir boundary conditions, viii) bottom layer: closed boundary conditions, ix) side walls: periodic boundary conditions; c) 3D view of a fraction of the spatial model, size of the spatial cell* $l_{sc} = 5\ \mu m$.

Observation: The graphical interface of the model shows data colected at the end of each time step (label 7iii in Figure 2.1). Figure 3.4 shows a screenshot of the graphical interface of the *v3D* version of the model. It is comprised by four graphical windows and a numeric display showing system-level variables that are updated on the fly. The windows represent (1) the temporal evolution of RBCs, and (2) merozoites and IRBCs, (3) the vertical cross-section of the hematocrit layer showing total number of RBCs, IRBCs, merozoites and packing factor for each stratum, and (4) the IRBC age structure. The numeric display (5) shows the number of time steps and equivalent time in real cultures, and the number of RBCs, IRBCs and extracellular merozoites.

Figure 3.4: *Screenshot of the version v3D of the model. This version oprates with a time step set to six minutes. The size of the spatial grid in this simulation is 20x20x60 spatial cells. The initial population is 24000 RBCs and the initial parasitaemia 1%. Windows show: 1) temporal evolution of RBC population (red line); 2) temporal evolution of parasitaemia parasitaemia (blue) and extracellmerozoites (grey); 3) vertical representation of the hematocrit layer: total number of RBCs (red), IRBCs (blue) and merozoites (green) per stratum; 4) age structure, histogram of the post invasion times among the IRBC subpopulation; 5) Numerical display showing the time step, number of RBCs, IRBCs and merozoites.*

Details

The *Initialization* and *External Inputs* in the version *v3D* are like those defined in 2D versions. Most of the *Submodels* also remain unchanged, except for: 1a) RBC Motion, 1d) RBC infection, 1e) RBC death, 2a) SC Diffusion and 2b) SC Propagation of extracellular merozoites. These modifications are the consequence of considering that the spatial cells

have a finite volume, that can be fill with RBCs, merozoites and the solid RBC remains that do not dissolve into the culture medium after cell lysis.

1a) RBC Motion. Appart from the processes described in Section 2.2, RBCs can now move through the hematocrit layer as a consequence of the settling process. Motion of RBCs may occur when there is enough room in the 9 spatial cells that comprise the nearest neighbours inmediatly below them. This shift of positions occurs with a fixed probability P_{fall}. Each RBC may fall one spatial cell, at most, per time step.

1d) RBC Infection. The infection process does not vary from the mechanism described in Section 2.2, except for three modifications:

i) merozoites are randamly distributed among one of the 27 nearest neighbour spatial cells, including the same cell. The probabilities of being dumped into each of the spatial cells are listed below. Same spatial cell (*i, j, k*): $P(1) = 0.33$, side-to-side cell (for instance (*i+1, j, k*)): $P(2) = 0.035$, immediate diagonal cell (for instance (*i+1, j +1, k*)): $P(3) = 0.025$, and double diagonal cell (for instance (*i+1, j+1, k*+1)): $P(4) = 0.02$ (See Figure 3.5).

ii) the extracellular merozoites can spread through the hematocrit layer during four time steps after merozoite eggress ($\sim$ 30 minutes). Each merozoite has a probability of moving to one of the nearest neighbour spatial cells in the level inmediatly below the present cell, at each time step. As for RBC motion, given that there is enough room, the probability of falling to any of the spatial cells is given by P_{fall} (see Figure 3.5).

iii) No limitations are imposed on the maximum number of parasites that can invade a healthy RBC.

Figure 3.5: *Stencils of the 3D models for: a) the eggress of merozoites at the end of the infection cycle; b) detail showing the four different tipe of neighbour cells (i.e. 1) same cell*

1e) RBC Death. After cell lysis the fraction of volume corresponding to solid unsolvable materials, wich represent approximately $V_{remain} = 6\ \mu m^3$ are left in the same spatial cell. At the end of each time step, just after merozoite propagation, these remains may fall to any of the nine nearest neighbour cells in the stratum inmediatly below, just like the RBCs do.

2a) SC Diffusion. Substrate diffusion is initially explicitly modelled with a FCTS as in Section 2.2.

$$C_{i,j,k}^{t+1} = C_{i,j,k}^{t} + \widetilde{D} \sum_{l,m,q}^{nn(i,j,k)} w_{l,m,q} C_{l,m,q}^{t} \tag{3.4}$$

l, m and *q* are the spatial coordinates of the 27 cells that constitute the inmediate environment of cell *(i,j,k)*. Equation 3.4 adds up the contributions of the each cell to the diffusive transport of substrate. The set of weights $w_{l,m,q}$ are:

$$w_{l,m,q} = \begin{cases} \frac{1}{2(6\sqrt{\frac{3}{2}}+3\sqrt{3}+4)} & ;\ 8\ \textit{cubic diagonals}:\ (l \neq i) \cap (m \neq j) \cap (q \neq k) \\ -1 & ;\ \textit{same spatial cell.}\ (l,m,q = i,j,k) \\ \frac{1}{2(\frac{6}{\sqrt{2}}+3+\frac{4}{\sqrt{3}})} & ;\ 12\ \textit{square diagonals, i.e.}\ (l \neq i) \cap (m \neq j) \cap (q = k) \\ \frac{1}{2(6+3\sqrt{2}+4\sqrt{\frac{2}{3}})} & ;\ 6\ \textit{square sides, i.e.}\ (l \neq i) \cap (m = j) \cap (q = k) \end{cases} \tag{3.5}$$

Substrate diffusivity is initially set to its maximum values $\widetilde{D} = 0.8$. This value is inadequate, and the submodel does not correctly account for diffusion, so it has been switched off in all the applications of INDISIM-RBC presented in this chapter. The problem regarding the model of diffusion is analyzed using other approaches in Section 3.5.2.

3.3 Analysis of experimental observations with the 3D model

3.3.1 Calibration of version *v3D*

The experimental results on the evolution of the parasitaemia for the short-term preservation (Pavanand et al., 1974) and long-term cultivation (Trager and Jensen, 1976) of *P. falciparum* in static *in vitro* cultures are used to calibrate the set of parameters employed by the model in the current version *v3D*.

The values for $\%I_0$, $\bar{t}_{INF}(t=0)$, P_{death} and P_{inf} are maintained to the ones used in version *2Dv.2* (see Sections 2.3.1 and 2.3.2). Two additional parameters are introduced